Check for updates

Geophysical Research Letters

RESEARCH LETTER
10.1029/2024GL110748

Relaxation States of Large Impact Basins on Mercury Based on MESSENGER Data

Claudia Szczech[1,2], Adrien Broquet[2], Ana-Catalina Plesa[2], Aymeric Fleury[2], Michaela Walterová[2,3], Alexander Stark[2], and Jürgen Oberst[1]

[1]Technical University of Berlin, Institute of Planetary Geodesy, Berlin, Germany, [2]German Aerospace Center (DLR), Institute of Planetary Research, Berlin, Germany, [3]Department of Geophysics, Faculty of Mathematics and Physics, Charles University, Prague, Czech Republic

Key Points:

- Observed Bouguer anomaly contrasts and predicted crustal temperatures are used to investigate viscoelastic relaxation of Mercury's basins
- Our findings do not indicate the anticipated pattern where basins exhibiting greater relaxation are situated in areas with hotter crust
- Crustal temperatures varied over time, likely due to rotation state changes or major volcanic events linked to smooth plain formation

Supporting Information:

Supporting Information may be found in the online version of this article.

Correspondence to:

C. Szczech,
Claudia.Szczech@dlr.de

Citation:

Szczech, C., Broquet, A., Plesa, A.-C., Fleury, A., Walterová, M., Stark, A., & Oberst, J. (2024). Relaxation states of large impact basins on Mercury based on MESSENGER data. *Geophysical Research Letters*, *51*, e2024GL110748. https://doi.org/10.1029/2024GL110748

Received 2 JUL 2024
Accepted 4 NOV 2024

Author Contributions:

Conceptualization: Claudia Szczech, Adrien Broquet
Data curation: Claudia Szczech
Formal analysis: Claudia Szczech, Adrien Broquet, Ana-Catalina Plesa, Alexander Stark
Funding acquisition: Jürgen Oberst
Investigation: Claudia Szczech, Adrien Broquet, Aymeric Fleury
Methodology: Claudia Szczech, Adrien Broquet
Resources: Jürgen Oberst
Software: Claudia Szczech, Aymeric Fleury
Supervision: Adrien Broquet, Ana-Catalina Plesa, Alexander Stark, Jürgen Oberst

© 2024. The Author(s).
This is an open access article under the terms of the Creative Commons Attribution License, which permits use, distribution and reproduction in any medium, provided the original work is properly cited.

Abstract The crustal structure of Mercury's large impact basins provides valuable insights into the planet's geological history. For a warm crust, a post-impact basin structure will viscously relax with inward flow of crustal materials toward the basin center. This effect drastically diminishes the crustal thickness contrasts and associated Bouguer gravity contrasts between the basin center and its surroundings. Here, we analyze Bouguer contrasts of 36 basins (diameter >300 km) located in the northern hemisphere as a proxy for viscoelastic relaxation. Thermal evolution models, assuming the present 3:2 spin-orbit configuration, are used to predict crustal temperatures. Our analysis reveals that the expected correlation between zones of warm crust and low Bouguer contrast from relaxation is not observed in the available data. This suggests that crustal temperatures have changed in the past, potentially due to a change in Mercury's orbit or to a major volcanic event associated with smooth plain formation.

Plain Language Summary Mercury's impact basins and their crustal structure provide important clues about the planet's geological past and present-day state. We study Mercury's crust at large impact basins by using information from gravity measurements and temperature estimates from thermal evolution models that consider the surface temperature pattern caused by Mercury's present-day orbit. In regions with warm interior, the crustal structure of large basins is expected to relax more readily compared to colder regions. Here, we examine 36 large basins (diameter >300 km) in the northern hemisphere, where the gravity data is well resolved, to investigate this process. Our results show no correlation between gravity data at basins' location, modeled local temperature, and expected impact basin relaxation. This suggests that crustal temperatures have changed in the past, potentially due to a change in Mercury's orbit or to a major volcanic event associated with smooth plain formation.

1. Introduction

Impact basins bear witness to the geologic history of celestial bodies. Their formation and evolution is profoundly connected to the thermal state of the crust and its evolution throughout geologic time (Melosh, 2011). Seconds after its formation and following the impact-driven excavation of crustal materials, an impact basin is characterized by a central depression and thinned crust (Melosh et al., 2013). Shortly after the impact, the central cavity is subject to an inward flow of surrounding crustal material. This flow might partially fill back the basin center, depending on the rheology and temperature of the crust (Miljković et al., 2013). The collapse of the transient crater leaves the basin in a pressure and gravitational disequilibrium, referred to as a subisostatic state. As the basin cools and forms a new lithosphere, the inner and outer parts of the basin are elevated back toward equilibrium due to isostatic forces. This coupled response causes the inner basin to experience uplift beyond isostasy and to form a mascon (Andrews-Hanna, 2013; Freed et al., 2014). The resultant thinned crust and uplifted mantle plug we observe today are typically expressed by topography-corrected gravity highs, hereafter referred to as positive Bouguer anomalies (Freed et al., 2014; Melosh et al., 2013; Neumann et al., 2015). Conversely, the basin's rim generally shows a negative Bouguer anomaly due to the local thickening of the crust by impact ejecta.

On the Moon, most basins on the nearside exhibit high Bouguer anomalies, which are primarily caused by dense volcanic mare infill (Broquet & Andrews-Hanna, 2024a). However, some non-mare basins also show elevated Bouguer anomalies, indicating the contribution of other factors, such as the flexural uplift of the crustal annulus (Andrews-Hanna, 2013). Alternatively, a large basin size, combined with high thermal gradients and low lithospheric rigidity, can result in a predominance of isostasy throughout the basin evolution, preventing the

Validation: Claudia Szczech, Adrien Broquet, Ana-Catalina Plesa, Michaela Walterová, Alexander Stark
Visualization: Claudia Szczech
Writing – original draft: Claudia Szczech
Writing – review & editing: Adrien Broquet, Ana-Catalina Plesa, Aymeric Fleury, Michaela Walterová, Alexander Stark

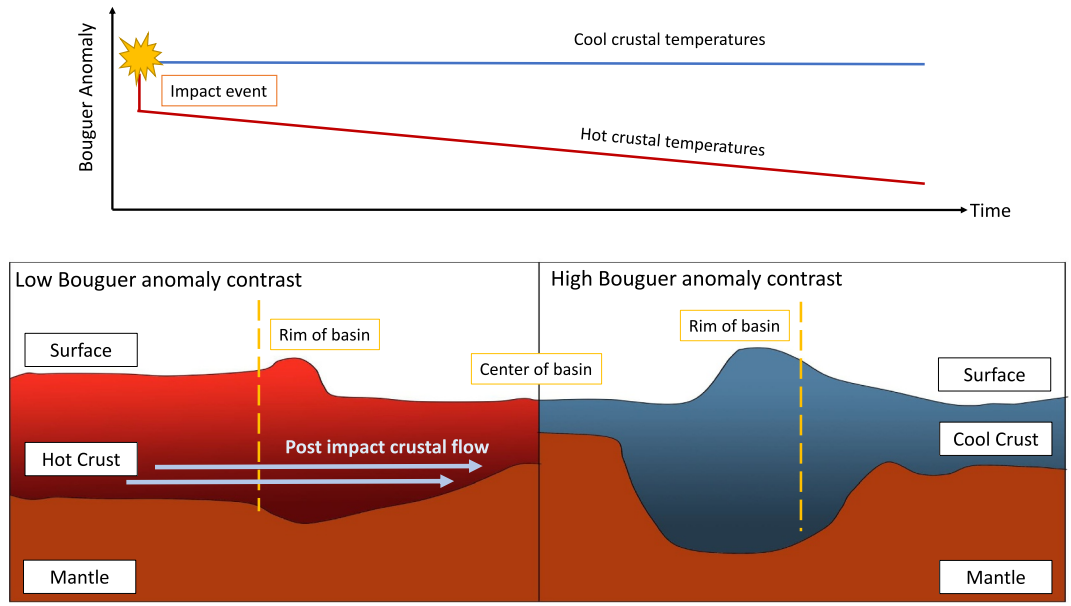

Figure 1. Sketch for the effect of crustal temperature on the relaxation state over time (top). Sketch of a post-impact structure profile within a hot crust (red) and a cool crust (blue). The yellow dashed line marks the impact structure rim. Light blue arrows indicate the post impact crustal flow.

development of a mascon with high Bouguer anomaly (Trowbridge et al., 2020). A comparable process may influence the gravitational signatures of large basins on Mercury.

In the case of a weak rheology or high sustained regional heat flow, the basic crustal structure described above can viscously relax leading to both reduction (or complete disappearance) of the thickened crustal annulus and further crustal flow toward the basin center (Ding & Zhu, 2022; Mohit & Phillips, 2006). These effects naturally lead to a drastic reduction of the crustal thickness contrast and associated Bouguer anomaly contrast between the basin center and surroundings. Simulations of Caloris formation reveal that a warm and weak interior enabled the crust to flow rapidly toward the basin center, suggesting Mercury was warmer than previously thought and that such thermal conditions drastically influence basin relaxation (Gosselin et al., 2023; Potter & Head, 2017). In that framework, analysis of Bouguer anomalies over large impact basins can be used to constrain the amount of post-impact crustal flow and relaxation. Together, these can help unravel the thermal state of the crust at the time of impact and the subsequent cooling history of the planet's interior (Figure 1; see also Mohit & Phillips, 2006; Deng et al., 2020).

Lacking in situ heat flow measurements and precise constraints on the composition and structure of the interior, the thermal evolution of Mercury is still only poorly understood (e.g., Michel et al., 2013; Tosi et al., 2013). Due to both the planet's proximity to the Sun and its peculiar 3:2 spin-orbit resonance (Bauch et al., 2021; Paige et al., 1992, 2012; Pettengill & Dyce, 1965), Mercury's surface is subject to substantial lateral variations in temperature reaching hundreds of Kelvins (Vasavada et al., 1999). Such temperature anomalies are expected to affect the deep thermal structure of the interior, potentially down to the planet's core (Tosi et al., 2015). Although these temperature anomalies prominently affected Mercury's thermal and geologic history, it remains unclear whether the 3:2 spin-orbit resonance is primordial, ancient, or recently acquired (Knibbe & van Westrenen, 2017; Noyelles et al., 2014; Wieczorek et al., 2012).

In this work, we analyze the Bouguer gravity anomalies of Mercury's largest impact basins as a proxy for the amount of viscoelastic relaxation experienced by these structures. In particular, we address whether the amount of viscoelastic relaxation these basin experienced is spatially correlated to the thermal effects of the 3:2 spin-orbit resonance. In the case where the resonance is primordial or ancient, large basins in zones of warm crust should be characterized by enhanced relaxation and low Bouguer anomaly contrasts. Patterns in Bouguer anomaly contrasts are compared to crustal temperature predictions from thermal evolution models that account for surface

19448007, 2024, 22, Downloaded from https://agupubs.onlinelibrary.wiley.com/doi/10.1029/2024GL110748 by Dtsch Zentrum F. Luft-U. Raum Fahrt In D. Helmholtz Gemein., Wiley Online Library on [17/11/2024]. See the Terms and Conditions (https://onlinelibrary.wiley.com/terms-and-conditions) on Wiley Online Library for rules of use; OA articles are governed by the applicable Creative Commons License

19448007, 2024, 22, Downloaded from https://agupubs.onlinelibrary.wiley.com/doi/10.1029/2024GL110748 by Dtsch Zentrum F. Luft-U. Raum Fahrt In D. Helmholtz Gemein., Wiley Online Library on [17/11/2024]. See the Terms and Conditions (https://onlinelibrary.wiley.com/terms-and-conditions) on Wiley Online Library for rules of use; OA articles are governed by the applicable Creative Commons License

temperature variations (Fleury et al., 2024). The results of this comparison are then used to discuss Mercury's orbital and rotational history.

2. Bouguer Anomaly and Mantle Temperature at Mercury's Largest Basins

In previous work, crustal thickness was utilized as a proxy for viscoelastic relaxation (Deng et al., 2020; Mohit, 2008). In particular, the difference in crustal thickness between the rim area and center of a basin (or crustal thickness contrast) was argued to represent a relative measure of the viscoelastic relaxation experienced by impact basins (Deng et al., 2020). Basins with a large crustal thickness contrast were interpreted as non-relaxed, whereas basins with a small contrast were considered to have experienced viscoelastic relaxation. Alternatively, the contrast in the Bouguer gravity anomaly has also been used as an indicator for viscoelastic relaxation (Johnson et al., 2018; Miljković et al., 2016; Mohit & Phillips, 2006, 2007; Potter et al., 2012). In this work, we focus on the Bouguer anomaly contrast, which doesn't require assumptions on the unknown density contrast at the crust-mantle interface, interface filtering, or average planetary crustal thickness (Beuthe et al., 2020).

In addition, previous studies have demonstrated that the basin diameter and morphology are highly dependent on the initial temperature of the crust (Miljković et al., 2013; Potter et al., 2012). Basins formed in a warm crust were approximately twice as large compared to those formed in a cooler crust under similar impact event conditions (Miljković et al., 2013). The collapse of the transient cavity was notably more prominent in larger and hotter basins compared to smaller basins or cooler crust. This process potentially led to the near-complete removal of crustal thickening regions, especially for the largest basins (Miljković et al., 2016). Taken together, an impact basin forming on a hot target should have drastically lower Bouguer gravity contrast, as due to post-impact flow and subsequent viscoelastic relaxation (Figure 1).

The Bouguer anomaly is estimated from the gravity field model of Goossens et al. (2022) and from elevation data derived by Perry et al. (2015) using the Mercury Laser Altimeter (MLA). We note that all gravity field solutions suffer from limited resolution on a global scale, specifically in the southern hemisphere, due to MESSENGER's highly inclined eccentric orbit (Solomon et al., 2018). As a result, this work specifically focuses on large basins located in the northern hemisphere, where the gravity field is sufficiently resolved. We use Mercury's basin inventory published by Szczech et al. (2024) and select 36 basins with a diameter >300 km located in the northern hemisphere from this catalog for our analysis.

To account for the variable resolution of the gravity field, we have pre-processed both the gravity and topography data by limiting their spectral expansion to a spatially variable maximum resolution (Broquet et al., 2024b). The spatially variable resolution is obtained from the local degree strength, which is defined as where the gravity signal of the coefficients of that degree equals the gravity uncertainty or noise (Konopliv et al., 2020). The Bouguer anomaly is computed using the *SHTools* python module (Wieczorek & Meschede, 2018) with a global flattening of 0.0009 and a mean global radius of 2,440 km (Konopliv et al., 2020). The Bouguer correction is applied, effectively removing the gravitational effects of surface topography between the observation point and the reference level, taking the elevation difference and the average density of the rocks above the reference level into account (Wieczorek, 2015). Our calculations assume a global crustal density of 2,800 kg m^{-3} (Genova et al., 2019, 2023; Goossens et al., 2022; Konopliv et al., 2020) and consider finite-amplitude corrections (see Section S1 in Supporting Information S1).

Impact basins are typically divided into three regions. The first region covers the central zone of crustal thinning and mantle uplift. It starts at the center of the impact structure and extends until a distance equal to half of the basin radius (Melosh, 2011; Neumann et al., 2015). The second region starts at half the basin radius and extends for another half radius, covering the area where the crust starts to thicken. The third region covers the rim crest and portions of the ejecta blanket of the impact structure over a distance equivalent to half of the basin radius. For this work, we calculate Bouguer anomaly profiles every 20° in azimuth, starting from the center of the basin and extending to a distance of 1.5 crater radius, and compute the mean value over the basin center and rim crest. The Bouguer anomaly contrast is defined as the difference between the basin center and the rim crest averages. In addition, we calculate the standard deviation to these mean values to evaluate our uncertainties.

To assess Mercury's crustal temperature and potential viscoelastic relaxation, we ran a suite of 3D thermal evolution models that include the effects of a spatially variable crustal thickness and surface temperature from Mercury's insolation pattern (Tosi et al., 2013; Vasavada et al., 1999). The heat producing elements, which are the

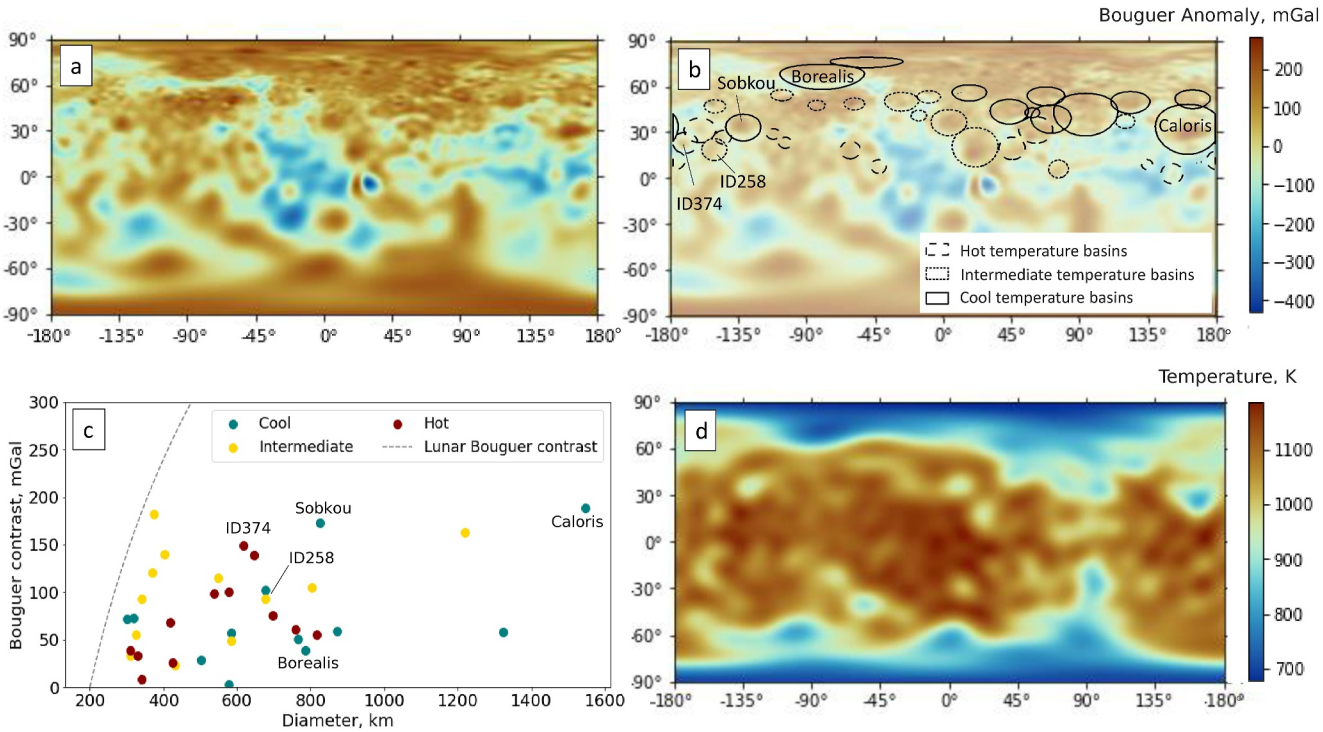

Figure 2. (a) Mercury's Bouguer anomaly map. (b) Same map as in panel (a) but including impact structure distribution of cool, intermediate, and high temperature at the basins' location. (c) Bouguer anomaly contrast versus basin diameter. The three temperature categories are indicated by colors. For reference, the gray dashed line shows the lunar Bouguer gravity diameter relationship from Neumann et al. (2015). (d) The temperature map at a depth of 40 km at 3 Ga obtained from a thermal evolution model of Mercury's interior (Fleury et al., 2024).

major source of interior heating, are distributed between the mantle and the crust following previous work (Fleury et al., 2024; Tosi et al., 2013). The models are run for 4.5 billion years and track the evolution of the interior temperature. Here, we focus on the temperature of the mantle below the crust at 40 km depth, which drives viscoelastic relaxation (Figure 2d and Ding & Zhu, 2022). We address the potential influence of small-scale temperature variations by converting the temperature map into spherical harmonics and selectively retaining only the low-degree coefficients up to degree and order 20. This approach allows us to focus on the long-wavelength temperature pattern, effectively minimizing the impact of small scale fluctuations. The temperature is estimated at 3 Ga, after the major basin-forming era (Orgel et al., 2020), though we note that the simulated overall temperature pattern remained similar throughout the entire simulation run of Mercury's evolution (Fleury et al., 2024). The crustal temperature is estimated for all basins by calculating profiles along the temperature map every 20° in azimuth and computing the mean value within one crater radii. Again, we derive the standard deviation to examine the uncertainties associated with our temperature estimates.

We note that factors such as lateral variability in radiogenic heat-producing elements, bulk porosity, and bulk crustal composition also potentially have a prominent effect on crustal temperatures and viscoelastic relaxation. However, these factors are often difficult to precisely constrain, unlike surface temperature.

When comparing Bouguer anomaly contrasts and analyzing the viscoelastic relaxation stages of impact basins, it is important to look for basins with similar ages. This ensures that our analysis does not compare old basins with much younger ones, the latter having less time to relax. To assess basin ages, we perform crater size frequency distribution measurements using the global catalog of craters provided by Herrick et al. (2018) (see Section S2 in Supporting Information S1). Our crater counting results are consistent with earlier work (Orgel et al., 2020).

3. Results

We classify the crustal temperature of Mercury's large basins according to tertile grouping (three groups, each containing a third of the population) as cool (<972 K), intermediate (972–1005 K) and hot (>1005 K, Figures 2b

19448007, 2024, 22, Downloaded from https://agupubs.onlinelibrary.wiley.com/doi/10.1029/2024GL110748 by Dtsch Zentrum F. Luft-U. Raum Fahrt In D. Helmholtz Gemein., Wiley Online Library on [17/11/2024]. See the Terms and Conditions (https://onlinelibrary.wiley.com/terms-and-conditions) on Wiley Online Library for rules of use; OA articles are governed by the applicable Creative Commons License

19448007, 2024, 22, Downloaded from https://agupubs.onlinelibrary.wiley.com/doi/10.1029/2024GL110748 by Dtsch Zentrum F. Luft-U. Raum Fahrt In D. Helmholtz Gemein., Wiley Online Library on [17/11/2024]. See the Terms and Conditions (https://onlinelibrary.wiley.com/terms-and-conditions) on Wiley Online Library for rules of use; OA articles are governed by the applicable Creative Commons License

and 2c). We note that the temperature map (Figure 2d) shows a similar pattern to the global Bouguer anomaly map (Figure 2a), which is likely linked to deep mantle thermal anomalies (Tosi et al., 2015).

In the case of little to no viscoelastic relaxation of the post-impact crustal structure of a basin, the Bouguer anomaly contrast of large basins is thought to be linearly proportional with their diameter, as observed on the cold lunar farside (Neumann et al., 2015). However, in case of a viscoelastically relaxed crust, this linear diameter scaling would be modified and Bouguer contrasts would be lower in regions with a warm interior and respectively higher in regions that are colder (Figure 2). Therefore, an inverse correlation between crustal temperature and the Bouguer contrast would indicate substantial viscoelastic relaxation. Our analysis of Bouguer anomalies show that basins on Mercury generally have smaller Bouguer contrast than found on the Moon when considering a similar diameter range. However, they follow a trend similar to the Moon at small diameters (around 300–400 km), with a slight offset. This offset can potentially be attributed to a larger density difference between the crust and mantle. Mercury's crust-mantle density contrast is approximately 400 kg m^{-3} (Genova et al., 2023), while the lunar density contrast is 700 kg m^{-3} (Wieczorek et al., 2013). For larger diameters, Mercury shows drastically lower Bouguer contrasts compared to the Moon. Large basins are more likely to experience relaxation and Bouguer contrast reduction, in particular basins with diameters >500 km (Figure 2c).

Relaxation could be more pronounced on Mercury due to its higher surface temperature, elevated radiogenic heating, and stronger gravitational acceleration, all of which enhance the flow and deformation of the crust over time. Importantly, we note that while the basin Bouguer contrast and diameter relationship is well defined on the Moon, the lack of high-resolution gravity data on Mercury makes the robust determination of such trend difficult. For this reason, and in order to limit the basin-diameter effect on the Bouguer contrast, we subdivided the basin population in 6 diameter ranges starting from 300 km to >800 km with increment of 100 km. Within these bins, relative variations in Bouguer contrast should be representative of the relative viscoelastic relaxation of the crustal structure.

For clarity, we focus here on three specific large basins with diameters of ~700 km that have similar ages and formed during the pre-Tolstojan and Tolstojan epochs (Figure 3). These basins, ID374, ID258 and ID270 (Borealis), are located in our three different temperature zones and in regions with sufficiently resolved gravity field (degree strength >30, wavelength >195 km). Interestingly, our analysis reveals no correlation between low Bouguer contrasts and hot regions, contrary to the expected relationship. Instead, a high Bouguer contrast is found in a region with hot crust (ID374), compared to a low contrast in a cool area (ID270, Figure 3). This unexpected positive correlation does emerge for the three specific basins in Figure 3, which warrants further investigation. No clear trend is observed in our entire database of large basins, with for example, highly relaxed basins being located in regions with cold crust (Figure 4). Neither a correlation on the global scale nor within specific diameter bin categories is evident.

On the Moon, Bouguer contrasts can be affected by mare basalts that have densities higher than the surrounding feldspathic crust $\Delta \sim 400$ kg m^{-3} (Kiefer et al., 2012). On Mercury, however, smooth plains are expected to have a density roughly similar to the surrounding crust (Beuthe et al., 2020). In addition, we have compared the depth of Borealis (2.2 km) to that of similarly sized basins devoid of smooth plains (ID114, ID276, ID108) and found only minor differences (depths of 1.9 km, 2.8 km, 1.8 km respectively). Therefore, based on this comparison, it is likely that the smooth plains within Borealis are thin (<0.6 km, Szczech, 2024). Together, these indicate that the effect of smooth plains on Bouguer anomalies is minor.

4. Discussion and Conclusions

All materials are subject to viscoelastic flow, the rate of which depends on temperature and rheology. The crustal structure of large basins on the terrestrial bodies, including the Moon (Ding & Zhu, 2022), Mars (Karimi et al., 2016; Mohit & Phillips, 2007), and Mercury (Deng et al., 2020) have been shaped by viscoelastic relaxation. Previous studies have suggested a relationship between crustal temperature and relaxation processes in impact structures (Deng et al., 2020). However, our analyses indicate that the expected relationship between our predicted crustal temperatures and observed Bouguer anomaly contrasts doesn't exist on Mercury. Instead, a size dependency was observed, with Bouguer anomalies tending to decrease for larger basins.

There are three primary scenarios for understanding Bouguer anomaly variations related to crustal temperature in impact basins. In the first scenario, a high Bouguer anomaly indicates that the basin formed in a cold crust, which

10.1029/2024GL110748

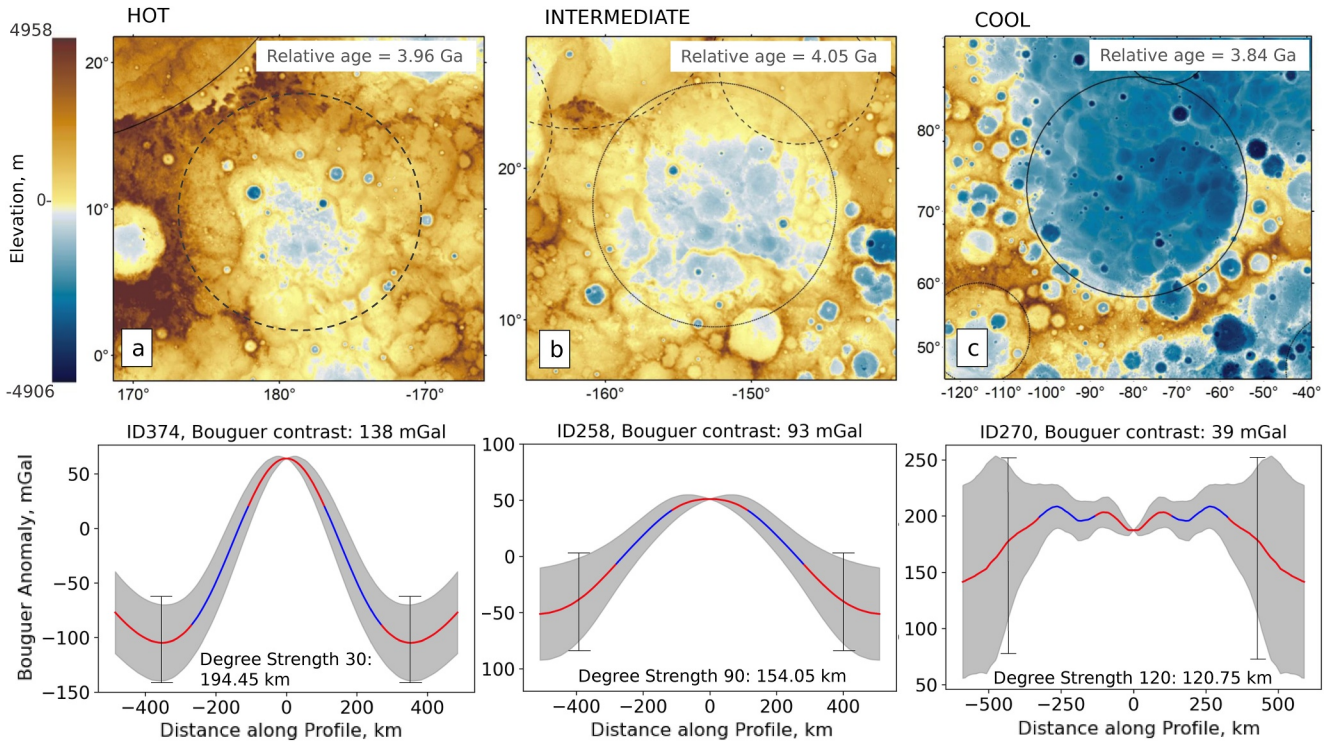

Figure 3. Characteristics of three example basins from our inventory. Local elevation (top) and average Bouguer anomaly profiles for each basin (bottom). Vertical bars mark the end of the basin rim. The relative age was determined using our crater counts and the chronology function of Neukum et al. (2001). The Bouguer contrast is the difference between the average of the rim crest and the basin's center (shown in red). (a) Basin ID374 is located in a hot temperature zone and has a high Bouguer anomaly contrast. (b) Basin ID258 (Budh) is located in an area of intermediate temperatures and has an intermediate Bouguer anomaly contrast. (c) Basin ID270 (Borealis) is located within a cool temperature zone and displays a low Bouguer anomaly contrast.

hinders relaxation allowing the basin to preserve a high Bouguer anomaly contrast. The second scenario involves a low Bouguer anomaly, suggesting the basin formed in a warmer region, facilitating viscous relaxation. The third scenario includes a basin that formed in a cold crust and was subsequently relaxed by a temperature increasing event, such as volcanism or a change in the planet's orbit.

Because of Mercury's spin-orbit resonance and the close proximity to the Sun, the planet's crustal temperature is substantially affected by the surface temperature (Tosi et al., 2015; Vasavada et al., 1999). Our thermal evolution models have used Mercury's surface temperature, as dictated by the current planetary 3:2 spin-orbit resonance. However, if this rotational configuration was not primordial or ancient, but rather recently acquired, this temperature pattern may not have affected the viscoelastic relaxation of our investigated large basins' crustal structure. This scenario requires the current planet's stable 3:2 spin-orbit resonance to postdate the formation of most large basins in the Tolstojan period (4.0–3.9 Gyr, Neukum et al., 2001; Orgel et al., 2020). Since viscoelastic relaxation is influenced by background heat flow and typically takes several tens to hundreds of millions of years to occur (Karimi et al., 2016; Mohit & Phillips, 2006), the current temperature pattern would need to have been established several hundred million years after the Tolstojan period to avoid altering the observed Bouguer anomalies.

Previous studies hypothesized that Mercury might have been initially locked in a different spin-orbit resonance, with 1:1 and 2:1 being the most likely candidates (Correia & Laskar, 2009; Correia & Laskar, 2010; Knibbe & van Westrenen, 2017; Noyelles et al., 2014; Wieczorek et al., 2012). According to this hypothesis, this early rotation state was later destabilized by a major impact, possibly associated with the formation of the Caloris basin. A different spin-orbit resonance would yield a different surface temperature pattern, which could help explain the distribution of Bouguer anomaly contrasts found in this study. The same would be true for a different orientation of the planet early in its history. What rotational and orbital evolutionary path could possibly explain our results is yet to be determined.

19448007, 2024, 22, Downloaded from https://agupubs.onlinelibrary.wiley.com/doi/10.1029/2024GL110748 by Dtsch Zentrum F. Luft-U. Raum Fahrt In D. Helmholtz Gemein., Wiley Online Library on [17/11/2024]. See the Terms and Conditions (https://onlinelibrary.wiley.com/terms-and-conditions) on Wiley Online Library for rules of use; OA articles are governed by the applicable Creative Commons License

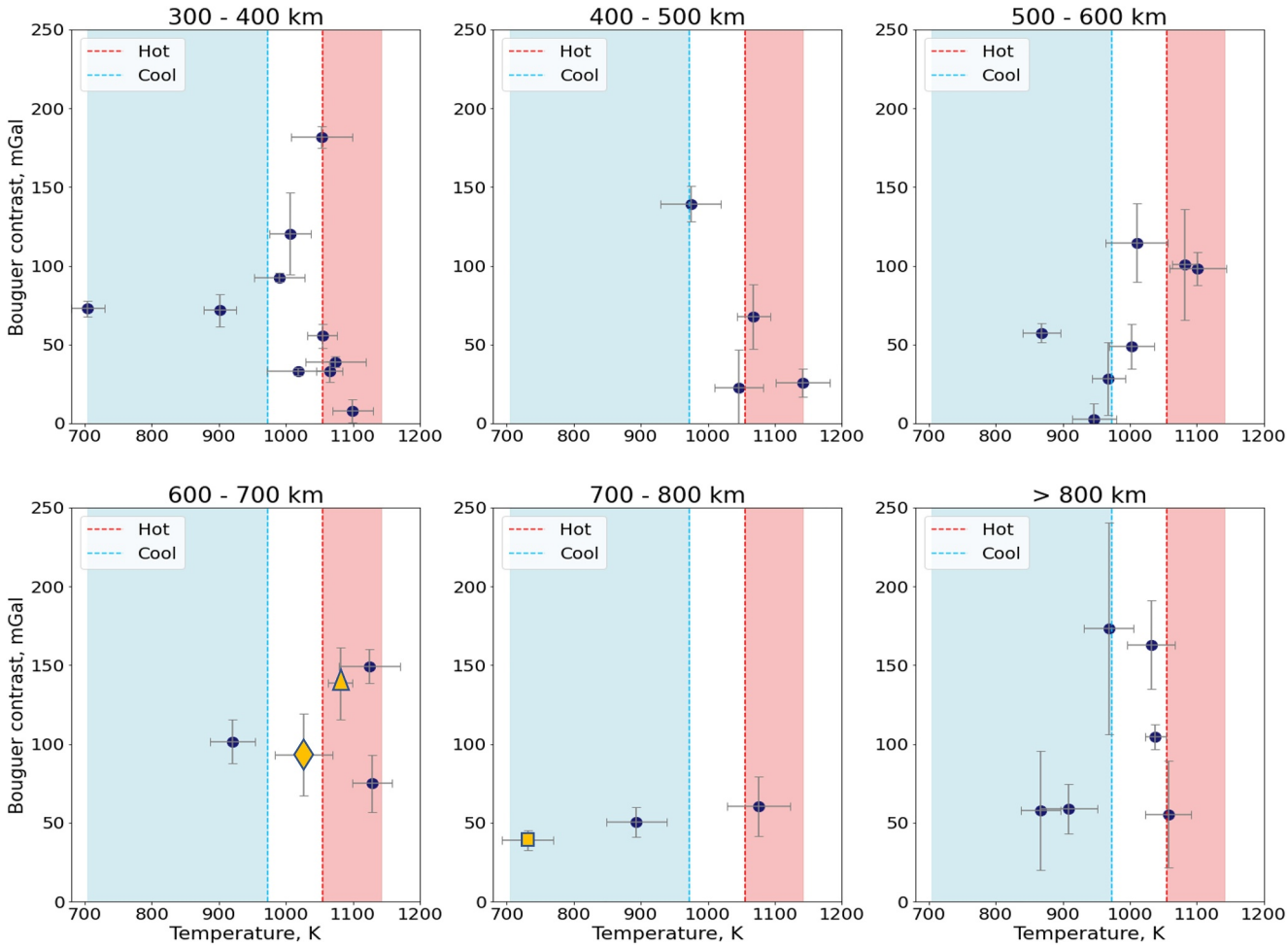

Figure 4. Bouguer anomaly contrast as a function of crustal temperature for several basin diameter ranges. All impact structures are located in the northern hemisphere, where the gravity field is sufficiently resolved. The light blue area marks the cool temperature zone, while the red area indicates the hot temperature zone. Gray vertical and horizontal bars denote the standard deviation for each parameter. The yellow triangle represents basin ID374, the diamond displays basin ID258, and the cube marks basin ID270 shown in Figure 3.

It is important to note that other factors may influence the Bouguer anomaly, such as density variations in the crust due to intrusions, and volcanic filling of basins as seen on the Moon (Broquet & Andrews-Hanna, 2024a, 2024b). Volcanic activity and magmatism might also largely affect the thermal structure of the crust and the associated evolution of a basin (Ding & Zhu, 2022). A major volcanic event leading to the formation of the smooth plains around 3.9–3.7 Ga (Denevi et al., 2013; Head et al., 2011) may have substantially affected Mercury's thermal evolution and crustal temperature at the time of large impact basins formation. Porosity also may influence Bouguer contrast, as demonstrated in lunar impact crater studies (Izquierdo et al., 2021; Soderblom et al., 2015). However, given that we focus on basins of similar sizes, impact-induced porosity should affect those equally. Therefore, the effect of porosity on the Bouguer contrast would be limited. In addition, the composition of the crust largely affects its rheology, and hence, its ability to flow. If the crust of Mercury was more mafic than felsic (silica-rich), viscoelastic relaxation may also be largely hindered, as discussed for ancient crustal plateaus on Venus (Nimmo & Mackwell, 2023) and in some studies of impact basins on the Moon (Mohit & Phillips, 2006).

The investigations presented here are the first to show the absence of a correlation between Bouguer anomaly contrast and crustal temperature, indicative of relaxation, for large impact basins on Mercury. This paves the way for future studies to test alternative evolutionary scenarios that may explain the absence of the expected trend, as discussed above. Additional numerical modeling would also help to investigate viscoelastic relaxation in more detail than was possible using the approach presented here.

19448007, 2024, 22, Downloaded from https://agupubs.onlinelibrary.wiley.com/doi/10.1029/2024GL110748 by Dtsch Zentrum F. Luft-U. Raum Fahrt In D. Helmholtz Gemein., Wiley Online Library on [17/11/2024]. See the Terms and Conditions (https://onlinelibrary.wiley.com/terms-and-conditions) on Wiley Online Library for rules of use; OA articles are governed by the applicable Creative Commons License

The low resolution of available gravity models restricts our analysis to the northern hemisphere. However, future improvements are expected with the data from the BepiColombo mission, which will enhance the global degree strength to around 45 after the first year of the mission (Iess et al., 2021). The new measurements will provide a resolution of approximately 383 km for gravity models and generate high-resolution elevation models of the planet (Benkhoff et al., 2010; Genova et al., 2021; Iess et al., 2009; Mangano et al., 2021; Thomas et al., 2021). Such higher resolution would enable the inclusion of 34 basins from the southern hemisphere, offering a more complete and detailed analysis of Mercury's viscoelastic relaxation processes. Such analyses will help to fill the gap in the comprehensive understanding of Mercury's crustal dynamics and improve the robustness of our results.

Data Availability Statement

The MESSENGER gravity and topography model can be accessed via https://pgda.gsfc.nasa.gov/data/MercuryCrust/sha.LOS_model and https://pds-geosciences.wustl.edu/messenger/mess-h-rss_mla-5-sdp-v1/messrs_1001/data/shadr/gtmes_150v05_sha.tab. The degree-strength downsampled topography is available at Broquet et al. (2024a). The catalogue of impact structures is available at Szczech (2024).

Acknowledgments
We thank Mike Sori and an anonymous reviewer for their insightful comments that helped to improve an earlier version of the paper, and the editor Kevin Lewis for handling our manuscript. C. S. is supported by the Deutsche Forschungsgemeinschaft (DFG) Grant SFB-TRR 170, Subproject A06. A. B. is funded by the Alexander von Humboldt Foundation. M. W. is supported by the Czech Science Foundation Grant 23-06513I. We thank the BELA Experiment teams at DLR (Institute of Planetary Research, Berlin) and at University of Bern (Physikalisches Institut, Bern) as well as the BELA Science Team. We also acknowledge the support by the BepiColombo project teams at ESTEC, ESOC, and ESAC. Open Access funding enabled and organized by Projekt DEAL.

References

Andrews-Hanna, J. C. (2013). The origin of the non-mare mascon gravity anomalies in lunar basins. *Icarus*, *222*(1), 159–168. https://doi.org/10.1016/j.icarus.2012.10.031

Bauch, K., Hiesinger, H., Greenhagen, B., & Helbert, J. (2021). Estimation of surface temperatures on Mercury in preparation of the MERTIS experiment onboard BepiColombo. *Icarus*, *354*, 114083. https://doi.org/10.1016/j.icarus.2020.114083

Benkhoff, J., Casteren, J. v., Hayakawa, H., Fujimoto, M., Laakso, H., Novara, M., et al. (2010). BepiColombo—Comprehensive exploration of Mercury: Mission overview and science goals. *Planetary and Space Science*, *58*(1), 2–20. https://doi.org/10.1016/j.pss.2009.09.020

Beuthe, M., Charlier, B., Namur, O., Rivoldini, A., & Van Hoolst, T. (2020). Mercury's crustal thickness correlates with lateral variations in mantle melt production. *Geophysical Research Letters*, *47*(9). https://doi.org/10.1029/2020GL087261

Broquet, A., & Andrews-Hanna, J. (2024a). The moon before mare. *Icarus*, *408*, 115846. https://doi.org/10.1016/j.icarus.2023.115846

Broquet, A., & Andrews-Hanna, J. (2024b). A volcanic inventory of the Moon. *Icarus*, *411*, 115954. https://doi.org/10.1016/j.icarus.2024.115954

Broquet, A., Rolser, F., Plesa, A.-C., Breuer, D., & Hussmann, H. (2024a). Data for Mercury's crustal porosity as constrained by the planet's bombardment history [Dataset]. *Zenodo*. https://doi.org/10.5281/zenodo.13938934

Broquet, A., Rolser, F., Plesa, A.-C., Breuer, D., & Hussmann, H. (2024b). Mercury's crustal porosity as constrained by the planet's bombardment history. *GRL: In Review*. https://doi.org/10.22541/essoar.171804829.91023526/v1

Correia, A. C., & Laskar, J. (2009). Mercury's capture into the 3/2 spin–orbit resonance including the effect of core–mantle friction. *Icarus*, *201*(1), 1–11. https://doi.org/10.1016/j.icarus.2008.12.034

Correia, A. C., & Laskar, J. (2010). Long-term evolution of the spin of Mercury: I. Effect of the obliquity and core–mantle friction. *Icarus*, *205*(2), 338–355. https://doi.org/10.1016/j.icarus.2009.08.006

Denevi, B. W., Ernst, C. M., Meyer, H. M., Robinson, M. S., Murchie, S. L., Whitten, J. L., et al. (2013). The distribution and origin of smooth plains on Mercury. *Journal of Geophysical Research: Planets*, *118*(5), 891–907. https://doi.org/10.1002/jgre.20075

Deng, Q., Li, F., Yan, J., Xiao, Z., Ye, M., Xiao, C., & Barriot, J.-P. (2020). The thermal evolution of Mercury over the past 4.2 Ga as revealed by relaxation states of mantle plugs beneath impact basins. *Geophysical Research Letters*, *47*(20), e2020GL089051. https://doi.org/10.1029/2020GL089051

Ding, M., & Zhu, M.-H. (2022). Effects of regional thermal state on the crustal annulus relaxation of lunar large impact basins. *Journal of Geophysical Research: Planets*, *127*(3). https://doi.org/10.1029/2021JE007132

Fleury, A., Plesa, A.-C., Tosi, N., Walterová, M., & Breuer, D. (2024). Variations of heat flux and elastic thickness of mercury from 3-d thermal evolution modeling. *Geophysical Research Letters*. https://doi.org/10.22541/essoar.172900776.60376472/v1

Freed, A. M., Johnson, B. C., Blair, D. M., Melosh, H. J., Neumann, G. A., Phillips, R. J., et al. (2014). The formation of lunar mascon basins from impact to contemporary form. *Journal of Geophysical Research: Planets*, *119*(11), 2378–2397. https://doi.org/10.1002/2014JE004657

Genova, A., Goossens, S., Del Vecchio, E., Petricca, F., Beuthe, M., Wieczorek, M. A., et al. (2023). Regional variations of Mercury's crustal density and porosity from MESSENGER gravity data. *Icarus*, *391*, 115332. https://doi.org/10.1016/j.icarus.2022.115332

Genova, A., Goossens, S., Mazarico, E., Lemoine, F. G., Neumann, G. A., Kuang, W., et al. (2019). Geodetic evidence that Mercury has A solid inner core. *Geophysical Research Letters*, *46*(7), 3625–3633. https://doi.org/10.1029/2018GL081135

Genova, A., Hussmann, H., Van Hoolst, T., Heyner, D., Iess, L., Santoli, F., et al. (2021). Geodesy, geophysics and fundamental physics investigations of the BepiColombo mission. *Space Science Reviews*, *217*(2), 31. https://doi.org/10.1007/s11214-021-00808-9

Goossens, S., Genova, A., James, P. B., & Mazarico, E. (2022). Estimation of crust and lithospheric properties for mercury from high-resolution gravity and topography. *The Planetary Science Journal*, *3*(6), 145. https://doi.org/10.3847/PSJ/ac703f

Gosselin, G. J., Freed, A. M., & Johnson, B. C. (2023). Crustal block and muted ring development during the formation of mercury's Caloris Megabasin. *Journal of Geophysical Research: Planets*, *128*(9). https://doi.org/10.1029/2023JE007920

Head, J. W., Chapman, C. R., Strom, R. G., Fassett, C. I., Denevi, B. W., Blewett, D. T., et al. (2011). Flood volcanism in the northern high latitudes of Mercury revealed by MESSENGER. *Science*, *333*(6051), 1853–1856. https://doi.org/10.1126/science.1211997

Herrick, R. R., Bateman, E. M., Crumpacker, W. G., & Bates, D. (2018). Observations from a global database of impact craters on mercury with diameters greater than 5 km. *Journal of Geophysical Research: Planets*, *123*(8), 2089–2109. https://doi.org/10.1029/2017JE005516

Herrick, R. R., Curran, L. L., & Baer, A. T. (2011). A Mariner/MESSENGER global catalog of Mercurian craters. *Icarus*, *215*(1), 452–454. https://doi.org/10.1016/j.icarus.2011.06.021

Iess, L., Asmar, S., Cappuccio, P. e. a., Cascioli, G., De Marchi, F., di Stefano, I., et al. (2021). Gravity, geodesy and fundamental physics with BepiColombo's MORE investigation. *Space Science Reviews*, *217*(21), 21. https://doi.org/10.1007/s11214-021-00800-3

Iess, L., Asmar, S., & Tortora, P. (2009). MORE: An advanced tracking experiment for the exploration of Mercury with the mission BepiColombo. *Acta Astronautica*, *65*(5–6), 666–675. https://doi.org/10.1016/j.actaastro.2009.01.049

19448007, 2024, 22, Downloaded from https://agupubs.onlinelibrary.wiley.com/doi/10.1029/2024GL110748 by Dtsch Zentrum F. Luft-U. Raum Fahrt In D. Helmholtz Gemein., Wiley Online Library on [17/11/2024]. See the Terms and Conditions (https://onlinelibrary.wiley.com/terms-and-conditions) on Wiley Online Library for rules of use; OA articles are governed by the applicable Creative Commons License

Izquierdo, K., Sori, M. M., Soderblom, J. M., Johnson, B. C., & Wiggins, S. E. (2021). Lunar megaregolith structure revealed by GRAIL gravity data. *Geophysical Research Letters*, *48*(22). https://doi.org/10.1029/2021GL095978

Johnson, B. C., Andrews-Hanna, J. C., Collins, G. S., Freed, A. M., Melosh, H. J., & Zuber, M. T. (2018). Controls on the formation of lunar multiring basins. *Journal of Geophysical Research: Planets*, *123*(11), 3035–3050. https://doi.org/10.1029/2018JE005765

Karimi, S., Dombard, A. J., Buczkowski, D. L., Robbins, S. J., & Williams, R. M. (2016). Using the viscoelastic relaxation of large impact craters to study the thermal history of Mars. *Icarus*, *272*, 102–113. https://doi.org/10.1016/j.icarus.2016.02.037

Kiefer, W. S., Macke, R. J., Britt, D. T., Irving, A. J., & Consolmagno, G. J. (2012). The density and porosity of lunar rocks. *Geophysical Research Letters*, *39*(7). https://doi.org/10.1029/2012GL051319

Knibbe, J. S., & van Westrenen, W. (2017). On Mercury's past rotation, in light of its large craters. *Icarus*, *281*, 1–18. https://doi.org/10.1016/j.icarus.2016.08.036

Konopliv, A., Park, R., & Ermakov, A. (2020). The Mercury gravity field, orientation, love number, and ephemeris from the MESSENGER radiometric tracking data. *Icarus*, *335*, 113386. https://doi.org/10.1016/j.icarus.2019.07.020

Mangano, V., Dósa, M., Fränz, M., Milillo, A., Oliveira, J. S., Lee, Y. J., et al. (2021). BepiColombo science investigations during cruise and flybys at the earth, Venus and mercury. *Space Science Reviews*, *217*(1), 23. https://doi.org/10.1007/s11214-021-00797-9

Melosh, H. J. (2011). *Planetary surface processes*. Cambridge Univ. Press.

Melosh, H. J., Freed, A. M., Johnson, B. C., Blair, D. M., Andrews-Hanna, J. C., Neumann, G. A., et al. (2013). The origin of lunar mascon basins. *Science*, *340*(6140), 1552–1555. https://doi.org/10.1126/science.1235768

Michel, N. C., HauckII, S. A., Solomon, S. C., Phillips, R. J., Roberts, J. H., & Zuber, M. T. (2013). Thermal evolution of Mercury as constrained by MESSENGER observations. *Journal of Geophysical Research: Planets*, *118*(5), 1033–1044. https://doi.org/10.1002/jgre.20049

Miljković, K., Collins, G. S., Wieczorek, M. A., Johnson, B. C., Soderblom, J. M., Neumann, G. A., & Zuber, M. T. (2016). Subsurface morphology and scaling of lunar impact basins. *Journal of Geophysical Research: Planets*, *121*(9), 1695–1712. https://doi.org/10.1002/2016JE005038

Miljković, K., Wieczorek, M. A., Collins, G. S., Laneuville, M., Neumann, G. A., Melosh, H. J., et al. (2013). Asymmetric distribution of lunar impact basins caused by variations in target properties. *Science*, *342*(6159), 724–726. https://doi.org/10.1126/science.1243224

Mohit, P. S. (2008). Viscous relaxation and early planetary evolution. *Eos, Transactions American Geophysical Union*, *89*(20), 185–186. https://doi.org/10.1029/2008EO200001

Mohit, P. S., & Phillips, R. J. (2006). Viscoelastic evolution of lunar multiring basins. *Journal of Geophysical Research*, *111*(E12). https://doi.org/10.1029/2005JE002654

Mohit, P. S., & Phillips, R. J. (2007). Viscous relaxation on early Mars: A study of ancient impact basins. *Geophysical Research Letters*, *34*(21). https://doi.org/10.1029/2007GL031252

Neukum, G., Oberst, J., Hoffmann, H., Wagner, R., & Ivanov, B. (2001). Geologic evolution and cratering history of Mercury. *Planetary and Space Science*, *49*(14), 1507–1521. https://doi.org/10.1016/S0032-0633(01)00089-7

Neumann, G. A., Zuber, M. T., Wieczorek, M. A., Head, J. W., Baker, D. M. H., Solomon, S. C., et al. (2015). Lunar impact basins revealed by gravity recovery and interior laboratory measurements. *Science Advances*, *1*(9), e1500852. https://doi.org/10.1126/sciadv.1500852

Nimmo, F., & Mackwell, S. (2023). Viscous relaxation as a probe of heat flux and crustal plateau composition on Venus. *Proceedings of the National Academy of Sciences of the United States of America* (Vol. 17(3), e2216311120). https://doi.org/10.1073/pnas.2216311120

Noyelles, B., Frouard, J., Makarov, V. V., & Efroimsky, M. (2014). Spin–orbit evolution of Mercury revisited. *Icarus*, *241*, 26–44. https://doi.org/10.1016/j.icarus.2014.05.045

Orgel, C., Fassett, C. I., Michael, G., Riedel, C., Bogert, C. H., & Hiesinger, H. (2020). Reexamination of the population, stratigraphy, and sequence of Mercurian basins: Implications for mercury's early impact history and comparison with the moon. *Journal of Geophysical Research: Planets*, *125*(8). https://doi.org/10.1029/2019JE006212

Paige, D. A., Siegler, M., Harmon, J., Neumann, G., Mazarico, E., Smith, D., et al. (2012). Thermal stability of volatiles in the north polar region of Mercury. *Science (New York, N.Y.)*, *339*(6117), 300–303. https://doi.org/10.1126/science.1231106

Paige, D. A., Wood, S. E., & Vasavada, A. R. (1992). The thermal stability of water ice at the poles of Mercury. *Science*, *258*(5082), 643–646. https://doi.org/10.1126/science.258.5082.643

Perry, M. E., Neumann, G. A., Phillips, R. J., Barnouin, O. S., Ernst, C. M., Kahan, D. S., et al. (2015). The low-degree shape of Mercury. *Geophysical Research Letters*, *42*(17), 6951–6958. https://doi.org/10.1002/2015GL065101

Pettengill, G. H., & Dyce, R. B. (1965). A radar determination of the rotation of the planet Mercury. *Nature*, *206*(4990), 1240. https://doi.org/10.1038/2061240a0

Potter, R. W. K., & Head, J. W. (2017). Basin formation on mercury: Caloris and the origin of its low-reflectance material. *Earth and Planetary Science Letters*, *474*, 427–435. https://doi.org/10.1016/j.epsl.2017.07.008

Potter, R. W. K., Kring, D. A., Collins, G. S., Kiefer, W. S., & McGovern, P. J. (2012). Estimating transient crater size using the crustal annular bulge: Insights from numerical modeling of lunar basin-scale impacts. *Geophysical Research Letters*, *39*(18). https://doi.org/10.1029/2012GL052981

Soderblom, J. M., Evans, A. J., Johnson, B. C., Melosh, H. J., Miljković, K., Phillips, R. J., et al. (2015). The fractured Moon: Production and saturation of porosity in the lunar highlands from impact cratering. *Geophysical Research Letters*, *42*(17), 6939–6944. https://doi.org/10.1002/2015GL065022

Solomon, S. C., Nittler, L. R., & Anderson, B. J. (2018). The MESSENGER mission: Science and implementation overview. In *Mercury: The view after messenger* (pp. 1–29). Cambridge University Press.

Szczech, C. C. (2024). Mercury's impact structure inventory [Dataset]. https://doi.org/10.5281/zenodo.11474513

Szczech, C. C., Oberst, J., Stark, A., Hussmann, H., & Preusker, F. (2024). Impact structures on Mercury from MESSENGER data: Implications on their formation processes and crustal structure. *Icarus*, *116244*, 116244. https://doi.org/10.1016/j.icarus.2024.116244

Thomas, N., Hussmann, H., Spohn, T., Lara, L. M., Christensen, U., Affolter, M., et al. (2021). The BepiColombo laser altimeter. *Space Science Reviews*, *217*(1), 25. https://doi.org/10.1007/s11214-021-00794-y

Tosi, N., Čadek, O., Běhounková, M., Káňová, M., Plesa, A.-C., Grott, M., et al. (2015). Mercury's low-degree geoid and topography controlled by insolation-driven elastic deformation. *Geophysical Research Letters*, *42*(18), 7327–7335. https://doi.org/10.1002/2015GL065314

Tosi, N., Grott, M., Plesa, A.-C., & Breuer, D. (2013). Thermochemical evolution of Mercury's interior. *Journal of Geophysical Research: Planets*, *118*(12), 2474–2487. https://doi.org/10.1002/jgre.20168

Trowbridge, A. J., Johnson, B. C., Freed, A. M., & Melosh, H. J. (2020). Why the lunar South Pole-Aitken Basin is not a mascon. *Icarus*, *352*, 113995. https://doi.org/10.1016/j.icarus.2020.113995

Vasavada, A. R., Paige, D. A., & Wood, S. E. (1999). Near-surface temperatures on Mercury and the Moon and the stability of polar ice deposits. *Icarus*, *141*(2), 179–193. https://doi.org/10.1006/icar.1999.6175

19448007, 2024, 22, Downloaded from https://agupubs.onlinelibrary.wiley.com/doi/10.1029/2024GL110748 by Dtsch Zentrum F. Luft-U. Raum Fahrt In D. Helmholtz Gemein, Wiley Online Library on [17/11/2024]. See the Terms and Conditions (https://onlinelibrary.wiley.com/terms-and-conditions) on Wiley Online Library for rules of use; OA articles are governed by the applicable Creative Commons License

Wieczorek, M. A. (2015). Gravity and topography of the terrestrial planets. In *Treatise on geophysics* (pp. 153–193). Elsevier. https://doi.org/10.1016/B978-0-444-53802-4.00169-X

Wieczorek, M. A., Correia, A., Feuvre, M. L., Laskar, J., & Rambaux, N. (2012). Mercury's spin–orbit resonance explained by initial retrograde and subsequent synchronous rotation. *Nature Geoscience*, *5*(1), 18–21. https://doi.org/10.1038/ngeo1350

Wieczorek, M. A., & Meschede, M. (2018). SHTools: Tools forWorking with spherical harmonics. *Geochemistry, Geophysics, Geosystems*, *19*(8), 2574–2592. https://doi.org/10.1029/2018GC007529

Wieczorek, M. A., Neumann, G. A., Nimmo, F., Kiefer, W. S., Taylor, G. J., Melosh, H. J., et al. (2013). The crust of the moon as seen by grail. *Science*, *339*(6120), 671–675. https://doi.org/10.1126/science.1231530

References From the Supporting Information

Fassett, C. I., Crowley, M. C., Leight, C., Dyar, M. D., Minton, D. A., Hirabayashi, M., et al. (2017). Evidence for rapid topographic evolution and crater degradation on Mercury from simple crater morphometry. *Geophysical Research Letters*, *44*(11), 5326–5335. https://doi.org/10.1002/2017GL073769

Wieczorek, M. A., & Phillips, R. J. (1998). Potential anomalies on a sphere: Applications to the thickness of the lunar crust. *Journal of Geophysical Research*, *103*(E1), 1715–1724. https://doi.org/10.1029/97JE03136

19448007, 2024, 22, Downloaded from https://agupubs.onlinelibrary.wiley.com/doi/10.1029/2024GL110748 by Dtsch Zentrum F. Luft-U. Raum Fahrt In D. Helmholtz Gemein, Wiley Online Library on [17/11/2024]. See the Terms and Conditions (https://onlinelibrary.wiley.com/terms-and-conditions) on Wiley Online Library for rules of use; OA articles are governed by the applicable Creative Commons License